frontiers | Frontiers in Earth Science

TYPE Original Research
PUBLISHED 03 August 2023
DOI 10.3389/feart.2023.1223939

OPEN ACCESS

EDITED BY
Andreas Franz Prein,
National Center for Atmospheric Research (UCAR), United States

REVIEWED BY
Kelly Nunez Ocasio,
National Center for Atmospheric Research (UCAR), United States
Dimitris Herrera,
The University of Tennessee, Knoxville, United States

*CORRESPONDENCE
Marni Pazos,
marni@unam.mx

RECEIVED 19 May 2023
ACCEPTED 24 July 2023
PUBLISHED 03 August 2023

CITATION
Pazos M, Magaña V and Herrera E (2023), Easterly wave activity in the Intra Americas Seas region analyzed with vertically integrated moisture fluxes. *Front. Earth Sci.* 11:1223939. doi: 10.3389/feart.2023.1223939

Easterly wave activity in the Intra Americas Seas region analyzed with vertically integrated moisture fluxes

Marni Pazos[1]*, Víctor Magaña[2] and Eduardo Herrera[3]

[1]Instituto de Ciencias de la Atmósfera y Cambio Climático, Universidad Nacional Autónoma de México, Mexico City, Mexico, [2]Instituto de Geografía, Universidad Nacional Autónoma de México, Mexico City, Mexico, [3]Facultad de Instrumentacion Electronica-Licenciatura en Ciencias Atmosfericas, Universidad Veracruzana, Xalapa, Veracruz, Mexico

Introduction: Easterly waves (EWs) are a dominant atmospheric phenomenon in the tropics. EWs in Mexico, Central America and the Caribbean region produce intense precipitation and significantly contribute to the summer rainy season, but some climatologies indicate their activity is weak or even null over the Intra-Americas Seas (IAS). As it is shown in the present study, EW activity over the IAS is not negligible but its variability is less than that off the western coast of Africa.

Method: Given the well-known coupling of wind and atmospheric moisture in EWs, their characteristics may be described using vertically integrated moisture fluxes (VIMF) and their divergence. By means of Hovmöller diagrams, lagged correlations and composite analyses, the propagation and the meteorological effects of these waves across the Caribbean Sea and the Gulf of Mexico, particularly on moisture and rains, are examined.

Results: It is observed that as EWs propagate, the VIMF convergence increases the level of precipitable water which frequently results in intense precipitation events. High frequency variability of the meridional component of the VIMF is used to estimate EW activity. Over the Caribbean Sea, EWs are less energetic than in the eastern tropical Atlantic even while the number of waves over these regions is comparable.

Discussion: When the Caribbean Low-Level Jet (CLLJ) is strong, EW activity tends to diminish due to a decrease in precipitable water (PW), sea surface temperature (SST) over the Caribbean, and possibly to an intensified vertical wind shear. Therefore, years of a stronger than normal CLLJ tend to result in summer precipitation below normal over most of the IAS and southern Mexico.

KEYWORDS

easterly waves, moisture fluxes, precipitation, Intra Americas Seas, extreme events

Introduction

The rainy season over most of Mexico, Central America and the Caribbean Sea occurs from June through October, with rain producing phenomena that include easterly waves (EWs) (e.g., Ladwig and Stensrud, 2009) and tropical cyclones (TCs) (e.g., Domínguez and Magaña, 2018). During the passage of these tropical systems subsidence is counterbalanced

by the corresponding ascending motion that, not only reduces the high stability of the region, but also act as important moisture transport mechanisms (Adams and Stensrud, 2007).

EWs are westward traveling atmospheric high-frequency transients in the easterlies (e.g., Riehl, 1945, 1948, 1954; Palmer, 1952; Tai and Ogura, 1987) and are precursors of more than half of the TCs in the North Atlantic (Avila et al., 2003; Núñez Ocasio and Rios-Berrios, 2023). EWs in the Atlantic may also lead to TCs in the eastern Pacific (e.g., Molinari et al., 2000). Furthermore, the rainy season in the tropical Americas or meteorological droughts may be influenced by EW activity (Méndez and Magaña, 2010; Gomes et al., 2015).

Early observational studies on tropical waves used spectral analysis and composite techniques to detect fluctuations in the wind field (Yanai et al., 1968; Nitta, 1970) and to characterize their wavelength and frequency (Burpee, 1974; Magaña and Yanai, 1991). In this way, it was determined that EWs have periods between 3 and 6 days, typical wavelengths between 2,500 and 4,000 km and propagate westward with a phase speed of 5–10 $m{\cdot}s^{-1}$ (Riehl, 1979; Wang, 2015). Over western Africa, the tropical Atlantic Ocean and the Caribbean Sea, their amplitude is larger at around 700 hPa and have a cold-core structure in the lower troposphere (Burpee, 1972, 1974; Reed et al., 1977; Thompson et al., 1979). EWs have a meridional extent of 10–15° with a west-east tilt between the surface and the mid-troposphere, and a southwest to northeast tilt in the axis of the inverted trough (Frank, 1969). Generally, low-level divergence, subsidence, and fair weather are observed ahead of the inverted trough axis in an EW, while convergence, ascending motion, a deep layer of moisture and disturbed weather are detected to the east of the trough axis of the wave (Carlson, 1969; Burpee, 1972).

Reed et al. (1988) found that EWs propagate from the west coast of Africa to the IAS following the mean low-level flow. Even more, some analyses indicate the EWs over the Caribbean region follow a southeast-northwest trajectory across the Gulf of Mexico (e.g., Kerns et al., 2008) and into the continent, influencing the North American Monsoon (Ladwig and Stensrud, 2009). Others have suggested that the preferred EW trajectories are from the Caribbean Sea into the eastern tropical Pacific (e.g., Serra et al., 2010). Various tracking schemes have been proposed to establish EW activity and the preferred EW trajectories. These EW detection schemes have led to construct climatologies (Thorncroft and Hodges, 2001; Hodges et al., 2003; Belanger et al., 2016; Lawton et al., 2022) which indicate that EW activity is minimum over the Caribbean given that not all African easterly waves reach the Caribbean Sea and the Gulf of Mexico (Enyew and Mekonnen, 2022), i.e., the Intra-Americas Sea (IAS) region (Maul, 2019). However, EWs are known to be an important element of weather in the region and an analysis to clarify this apparent contradiction should be conducted.

Humidity and stability across the tropical Atlantic are key factors that maintain EWs as they propagate from Africa into the Caribbean region, where the coupling between the wind field and convective activity constitutes a basic element for these disturbances to maintain their structure, as observed in satellite images (Molinari et al., 1997; Shelton, 2011). It has been suggested that EWs over the Caribbean Sea may intensify through wave mean flow interaction with the barotropically unstable Caribbean Low-Level Jet (CLLJ) (e.g., Molinari et al., 1997; Méndez and Magaña, 2010). Consequently, the characteristics of the mean low-level atmospheric flow in the Caribbean when EW activity is examined.

EWs result in periodic wet or dry episodes during the summer season and their activity may result in a weak or intense rainy season in the Mexico, Central America, and the IAS region (e.g., Hosler, 1956; Fuller and Stensrud, 2000; Ladwig and Stensrud, 2009). Determining the factors that control the interannual variability of EW activity may serve to produce better seasonal climate outlooks for the region. In addition, experienced meteorologists consider EWs as precursors of intense storms (e.g., reports in La Revista de Yucatán, 2023). Even more, the role of EW in inducing intense precipitation events that significantly contribute to seasonal rains, for instance in the African region, has been documented (e.g., Seo et al., 2008; Suneetha, 2018; Camberlin et al., 2020).

Therefore, the objective of the present study is to examine EW activity in the IAS region, its relationship to the mean atmospheric flow and the role of EWs as intense precipitation events precursors, examining their propagation from the Atlantic Ocean into the IAS and their role as a moisture transport mechanism.

Data

Numerous observational analyses to detect EWs and other type of tropical waves have been developed using wind data from atmospheric soundings (e.g., Yanai and Nitta, 1967) and reanalysis (e.g., Serra et al., 2010). Wind and moisture data at low tropospheric levels, serve to document the presence of EWs, which are also detected referring to the vertical component of the relative vorticity (Reed et al., 1988; Hodges et al., 2003; Belanger et al., 2016). Other analyses on EWs are based on satellite images (METED, 2023) or radar data (e.g., Cifelli et al., 2010).

The ERA-Interim data constitute an adequate source of gridded daily wind and atmospheric moisture data with high spatial resolution (0.75° × 0.75°) at various tropospheric levels, including 1,000, 925, 850, 700, and 500 hPa for the 1979–2018 period. In the present analysis, the ERA Interim data set is used to investigate the high frequency variance of the meridional component of the wind at 700 hPa (v_{700}). To estimate the coupling between wind and moisture in EWs, the vertically integrated moisture flux (VIMF) is calculated from the wind and moisture fields from 1,000 to 500 hPa.

VIMF is estimated using the expression:

$$VIMF = \frac{1}{g}\int_{p=1000}^{p=500} \boldsymbol{V} q \, dp \tag{1}$$

where q is the specific humidity ($kg{\cdot}kg^{-1}$), $\boldsymbol{V}$ is the horizontal wind field, g is the gravity constant, and p is the pressure between the 1,000 and 500 hPa. VIMF units are $kg{\cdot}m^{-1}{\cdot}s^{-1}$.

The VIMF is a measure of the amount of water vapor transported in the atmosphere and is frequently used along with its convergence to document hydrological processes in the atmosphere (Fasullo and Webster, 2003). The timing, position, and duration of high VIMF convergence zones may result in intense convective activity. The VIMF may also be used to examine moisture transport processes, for instance in EWs.

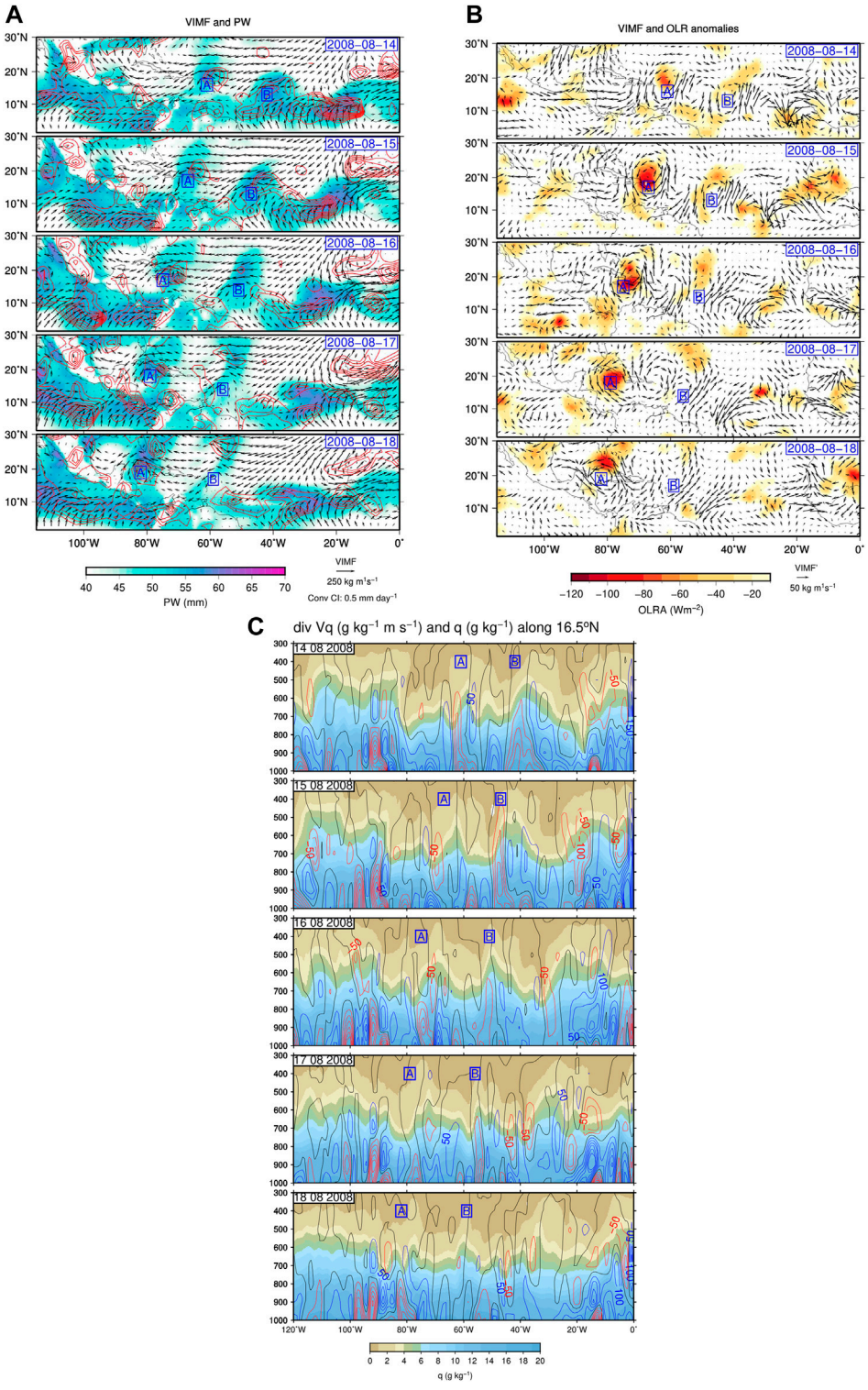

FIGURE 1
(A) Daily VIMF (vectors), VIMF convergence (contour interval: 0.5 mm day^{-1}) (red lines) and PW (shades of blue to magenta) for the period between 14/08/2008 (top) and 18/08/2008 (bottom). The A and B blue letters in squares correspond to inverted troughs associated with an EW train over the tropical Atlantic. **(B)** Daily high frequency (3–10 day)$^{-1}$ anomalies of VIMF (vectors) for zonal wave numbers (6–15) and negative OLR anomalies (shades of red to yellow) between 14/08/2008 (top) and 18/08/2008 (bottom). The A and B blue letters in squares correspond to the inverted troughs identified in **(A)**. **(C)** Vertical cross section along 16.5°N of daily specific humidity (shades of blue to brown) and moisture flux divergence (blue lines) and convergence (red lines) (contour interval 50 g·kg^{-1}·ms^{-1}) between 14/08/2008 (top) and 18/08/2008 (bottom). The A and B blue letters in squares correspond to the inverted troughs identified in **(A)**.

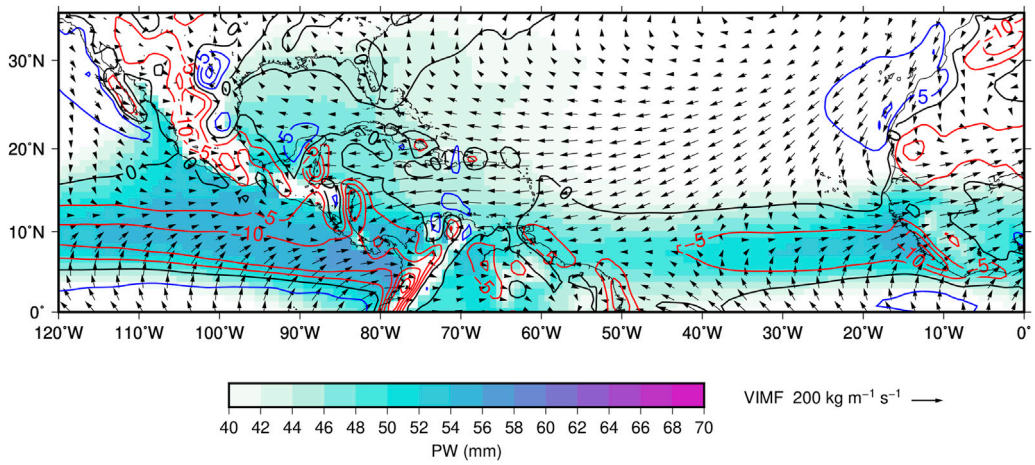

FIGURE 2
June-September climatology of the VIMF (kg·m^{-1}·s^{-1}) between 1,000 and 500 hPa (vectors), the VIMF divergence (contour interval 5 mm day^{-1}) (blue lines) and convergence (red lines), and PW larger than 40 mm (shades of blue and magenta).

The atmospheric moisture conservation equation for a vertical column is

$$\frac{\partial PW}{\partial t} = E - P - \frac{1}{g}\int_{1000}^{500} \nabla \cdot \boldsymbol{V} q \, dp \qquad (2)$$

and it describes temporal changes in precipitable water (PW) due to evaporation, *E*, precipitation, *P*, and to the moisture flux divergence (convergence). The VIMF convergence is calculated by numerically integrating VIMF fields between 1,000 and 500 hPa.

An atmospheric moisture-VIMF convergence (divergence) region is a moisture sink (source) region where PW tends to increase (decrease). Therefore, the intensity in VIMF convergence is important to understand the occurrence of extreme weather events, such as intense precipitation in hurricanes (e.g., Ejigu et al., 2021). The convergence of the VIMF and the increases in PW induced by EWs are considered significant modulators of precipitation over the IAS (Banacos and Schultz, 2005; Magaña and Díaz, 2022).

PW daily data is also obtained for the same period from the ERA Interim database and is evaluated using the atmospheric moisture content between 1,000 and 300 hPa by means of the expression.

$$PW = \frac{1}{g}\int_{1000}^{300} q \, dp \qquad (3)$$

Although PW considers the entire atmospheric column, the largest contribution to PW during the passage of an EW comes from moisture convergence at low atmospheric levels (below 500 hPa) (Burpee, 1974).

Daily Outgoing Longwave Radiation (OLR) data from the NOAA/NCEP are used to document deep convective activity in relation to EWs. The daily OLR data for the period 1981–2018 have a spatial resolution of 2.5° × 2.5° (Liebmann and Smith, 1996). Daily precipitation data from the National Water Commission (CONAGUA, 2023) station network over the eastern coast of the Yucatan Peninsula are used to identify intense precipitation events (>30 mm day^{-1}) during the passage of EWs.

Methodology

Tropical wave activity may be estimated by means of the high frequency variance of the meridional component of the wind (e.g., Magaña and Yanai, 1991) that reflects part of the perturbation kinetic energy (PKE) of a transient. Similar high frequency variance analyses of PW reflect the modulating effect of EWs in the moisture field. High frequency variability of PW and the meridional component of the VIMF ($VIMF_y$) are used to detect EW activity, considering the strong coupling of these variables for instance, in the rear of the inverted trough. Spectral analysis of the wind field, PW and $VIMF_y$ are used to obtain the frequency range that corresponds to the EWs signal across the Atlantic Ocean. The spectral analyses scheme by Olafsdottir et al. (2016) includes a significance test to detect significant variance as the one related to EWs in the high frequency period range.

Once the signals of EWs are detected, a band-pass filter (Murakami, 1979) is applied to the wind, PW and the VIMF fields to enhance their temporal characteristics. Composite VIMF patterns are prepared using band-pass filtered data based on indices related to EWs activity and dates of events of more than 30 mm day^{-1} to examine their characteristic temporal evolution.

Belanger et al. (2016) used wind data and other meteorological variables (e.g., relative vorticity) to characterize EWs over the tropical Atlantic Ocean. For instance, they document an EW event for 15 August 2008, over the tropical Atlantic. VIMF is an adequate variable to represent EWs, along with VIMF convergence, PW and OLR anomalies. The EW of August 15-19, 2008, over the Atlantic is detected as it propagates from western Africa into the

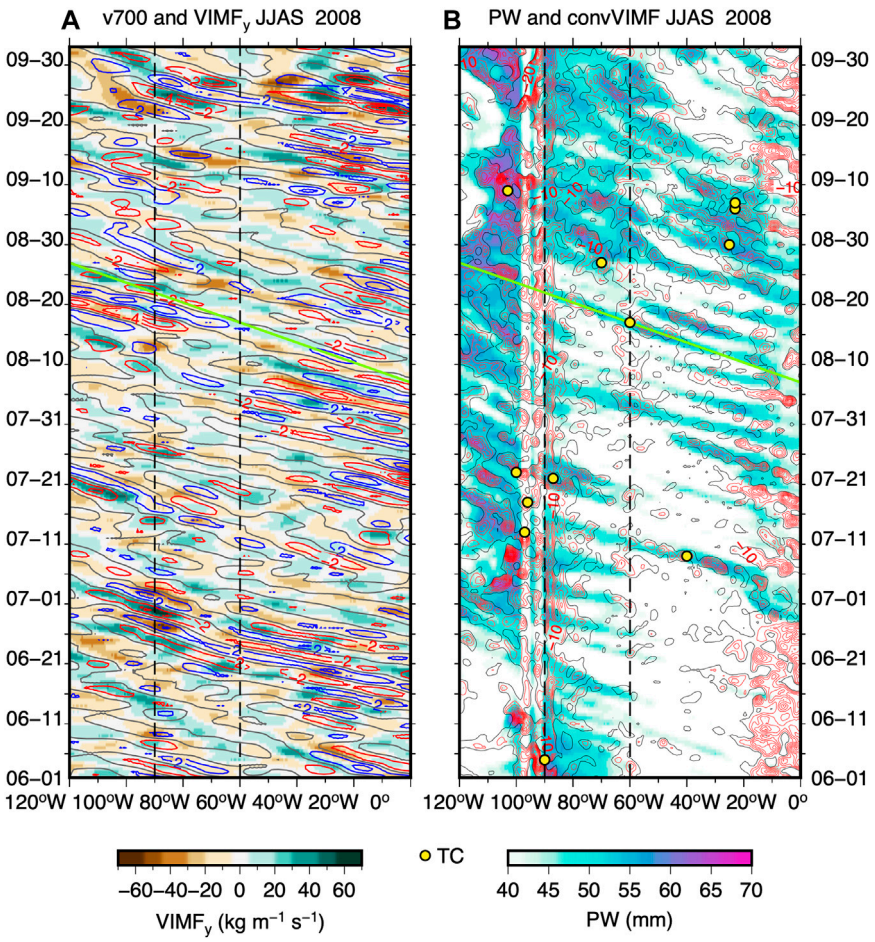

FIGURE 3
Hovmöller diagrams along 17°N for the eastern Pacific and tropical Atlantic of **(A)** high frequency anomalies of v_{700} (contour interval 2 m·s^{-1}; red and blue contours correspond to negative and positive values) and VIMF$_y$ (shades of brown and green), and **(B)** convergence of VIMF (red lines and contour interval: 5 mm day^{-1}) and values of PW larger than 40 mm (shades of blue-magenta), for the summer of 2008. The tilted green line shows the signal of the EW presented in Figure 1. Vertical dashed lines correspond to the Caribbean Sea longitudes. Yellow circles correspond to Tropical Cyclones.

Caribbean Sea (Figure 1). The inverted troughs (A and B) are associated with a tropical wave train in the VIMF field, where VIMF convergence and PW are large (Figure 1A). The corresponding anomalies in the VIMF and OLR fields indicate that the cyclonic (anticyclonic) circulation sequence in the EW result that modulates intense (null) tropical convection over the region (Figure 1B). A vertical cross-section of specific humidity and moisture flux convergence between 14 August and 18 August 2008 (Figure 1C) shows that the passage of the easterly wave train (indicated with letters A and B) modulates moisture flux convergence and divergence at low tropospheric levels and up to 700 hPa. Moisture flux convergence results in relatively large values of specific humidity from surface up to 500 hPa that reflects in large values of PW and VIMF convergence in locations A and B, as shown in Figure 1A.

The spatial patterns observed in Figures 1A, B are identifiable in lagged correlation analysis between a reference point in the central Caribbean and the rest of the domain and serve to examine the propagation of easterly waves over the IAS.

Results

Detecting EW activity over the IAS

From June through September, the VIMF is intense over most of the northern side of the Inter-Tropical Convergence Zone (ITCZ) in the Atlantic Ocean, around 10°N (Figure 2), with a dominant zonal component where trade winds are strong (>8 m·s^{-1}) where PW is larger than 40 mm. The combined effect of lower tropospheric winds and atmospheric moisture is represented in the VIMF fields, which show a magnitude close to 200 kg·m^{-1}·s^{-1} over most of the Caribbean Sea, in relation to the presence of the CLLJ. The low-level winds from the Atlantic Ocean transport moisture into the Caribbean Sea and at times, into the eastern tropical Pacific (Magaña and Díaz, 2022) and into the Gulf of Mexico. The divergence of the VIMF over the eastern-central Caribbean Sea is equivalent to 5 mm day^{-1} and constitutes a moisture source that contrasts with the intense moisture convergence (sink) in the CLLJ exit region, of up to −15 mm day^{-1}, off the Caribbean coast of Nicaragua, which results in large values of PW (>48 mm) and

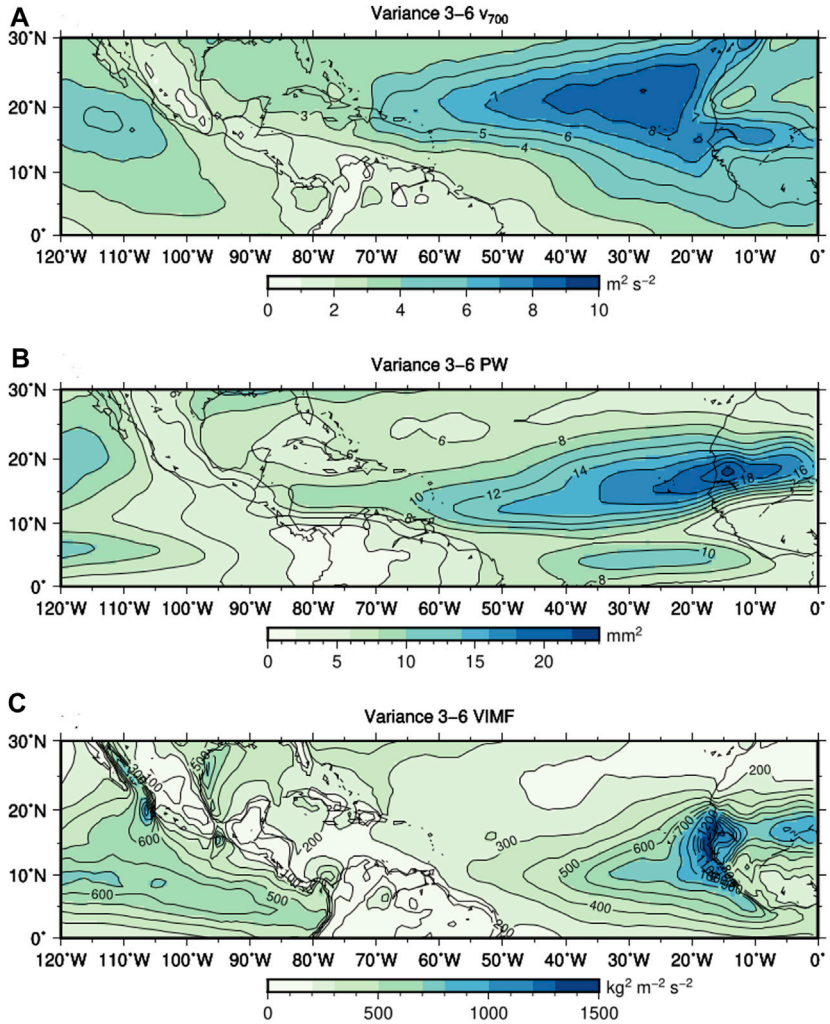

FIGURE 4
Variance in the 3–6 days period range for **(A)** for v_{700}, **(B)** for PW, and **(C)** for the meridional component of the VIMF, corresponding to the June-September period between 1979 and 2018.

precipitation (>10 mm day^{-1}). Convergence of the VIMF is larger (<−10 mm day^{-1}) over the eastern Pacific ITCZ, where the mean PW is more than 55 mm during summer. The southeast-northwest direction of the VIMF over the Gulf of Mexico constitutes a mean of moisture transport from the Caribbean Sea to northeastern Mexico and southern Texas. However, the divergence of the VIMF over the latter maintains semi-arid conditions, only interrupted by the passage of atmospheric transients such as EWs or tropical cyclones.

High frequency perturbations in the VIMF fields mainly correspond to EW activity in the tropical Atlantic and may be detected as fluctuations in the wind field at 700 hPa (Diedhiou et al., 1999), by tracking vorticity centers either at 600 or 850 hPa (Throncroft and Hodges, 2001), or by including analyses of changes in the atmospheric moisture fields or convective activity (brightness temperature anomalies) (e.g., Belanger et al., 2016). The moisture content in EWs is particularly important to maintain these tropical systems as they approach to the IAS. This reflects in intense convective activity (OLR negative anomalies), where large values of PW, VIMF and its convergence are present.

During the summer of 2008, high frequency (less than 10 days period) anomalies in the meridional wind at 700 hPa (v_{700}) or in $VIMF_y$ along 17°N may be used to detect EW activity across the Atlantic and eastern tropical Pacific (Figure 3A). EWs weaken near the Caribbean Sea, as observed in the amplitude of v_{700}. This weakening shows in EW climatologies (e.g., Thorncroft and Hodges., 2001). The EW signal in PW above 40 mm and in the convergence of the VIMF shows that most of the eastward propagating systems tend to extend across the Atlantic (Figure 3B) at a speed of the order of 6 ms^{-1} (green line in Figure 3), within the range of EW phase speed (Wang, 2015). However, not all African easterly waves reach the Caribbean Sea, particularly those with low atmospheric moisture transport and PW. Even more, some signals of EWs appear over the Caribbean and propagate into the eastern Pacific.

In general, African easterly waves that reach the IAS maintain their phase speed and coupling with the moisture field. Some African easterly waves do not reach the IAS since they become TCs and consequently, they do not add to the account of transients, making a difference between African wave activity and EW activity over the IAS. At times, it is observed that the signal of an EW begins

10.3389/feart.2023.1223939

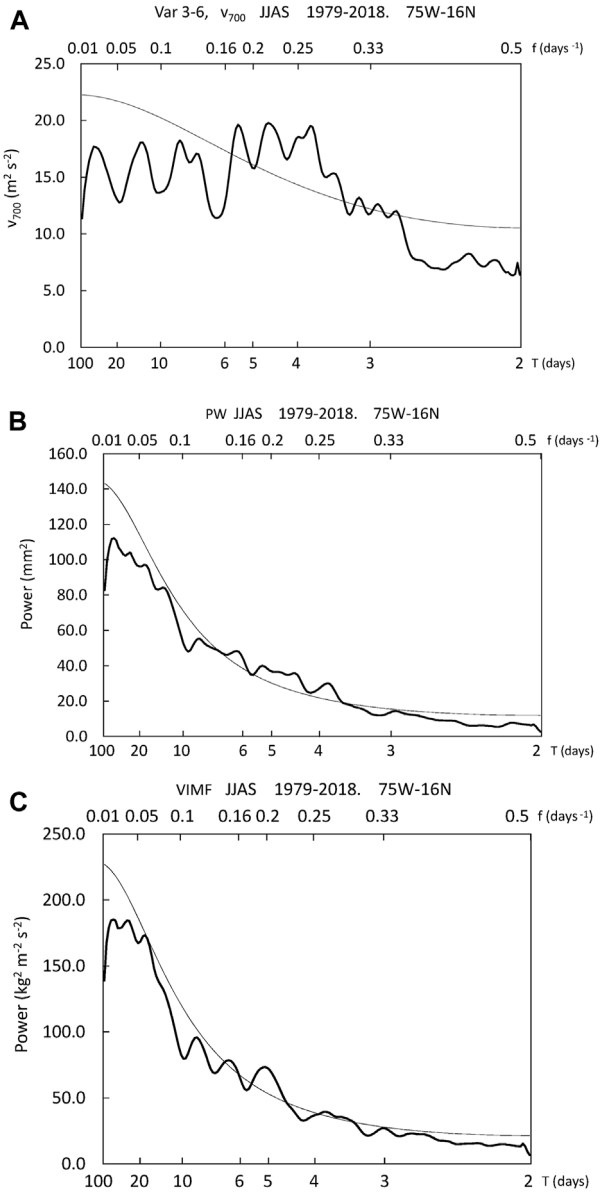

FIGURE 5
Power spectra, **(A)** for v_{700}, **(B)** for PW, and **(C)** the meridional component of the VIMF ($VIMF_y$). The spectral analyses are calculated for the June-September period of the years between 1979 and 2018, at 75°W, 16°N. The thin solid line indicates the 95% significance level.

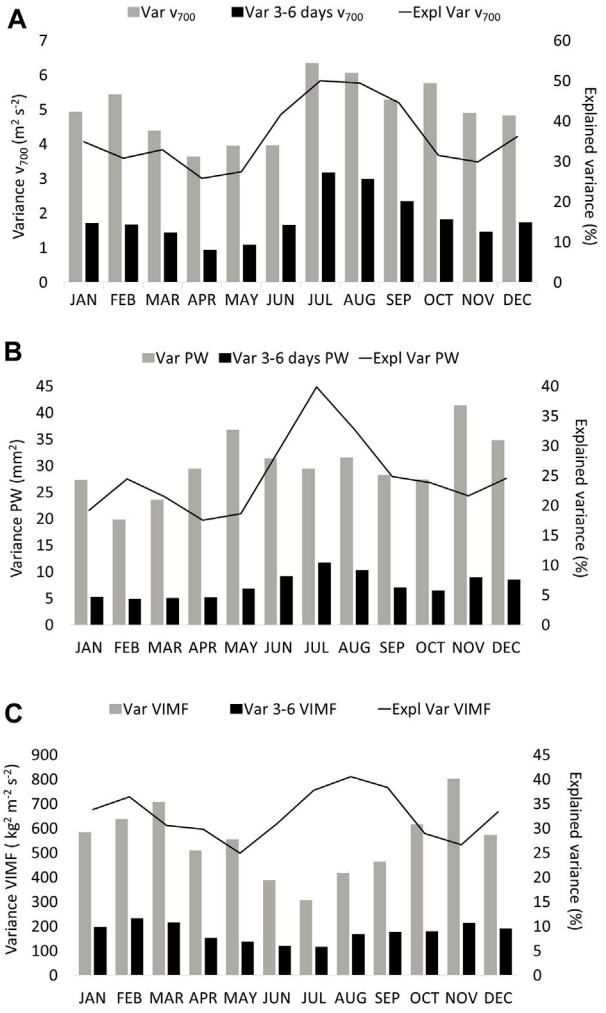

FIGURE 6
Monthly total (gray bar) and high frequency (3–6 days) (black bar) variance **(A)** of v_{700} ($m^2 \cdot s^{-2}$), **(B)** of PW (mm^2) and **(C)** of $VIMF_y$ ($kg^2 \cdot m^{-2} \cdot s^{-2}$), in the central Caribbean Sea (75°W, 16.5°N). The solid line corresponds to the explained (%) variance by high frequency transients.

slightly to the east of the Lesser Antilles and enhances over the IAS (Figure 3B). EWs in the eastern tropical Pacific may have a different origin (Whitaker and Maloney, 2020).

High frequency variability in the atmospheric circulations and EWs

From June through September, high frequency variability in v_{700} is commonly associated with African easterly waves or EWs in the Atlantic. The high frequency variance in v_{700} corresponds to a part of high frequency component of the PKE of EWs. It is large off the western coast of Africa and across the Atlantic and tends to diminish over the Caribbean Sea (Figure 4A). The high-frequency variance of PW (Figure 4B) and $VIMF_y$ (Figure 4C) is also large off the western coast of Africa and weaker over the IAS. The spatial distribution of high frequency PKE is related to EW activity and is like various EW climatologies (e.g., Belanger et al., 2016).

Although the high frequency variance related to EWs activity diminishes over the Caribbean Sea, the number of these tropical systems in this region is comparable to the number of African easterly waves (Frank, 1970; NHC 2022; http://www.nhc.noaa.gov/climo/; Trinidad and Tobago Weather Center https://ttweathercenter.com/2022/05/01/tropical-waves/, retrieved 25 March 2023), i.e., around 20 systems from June through September (Thorncroft and Hodges, 2001). The amplitude of v_{700} and the $VIMF_y$ fluctuations associated with EWs is at least four times larger over the western part of Africa than over the Caribbean Sea (Figure 4). Therefore, EW climatologies

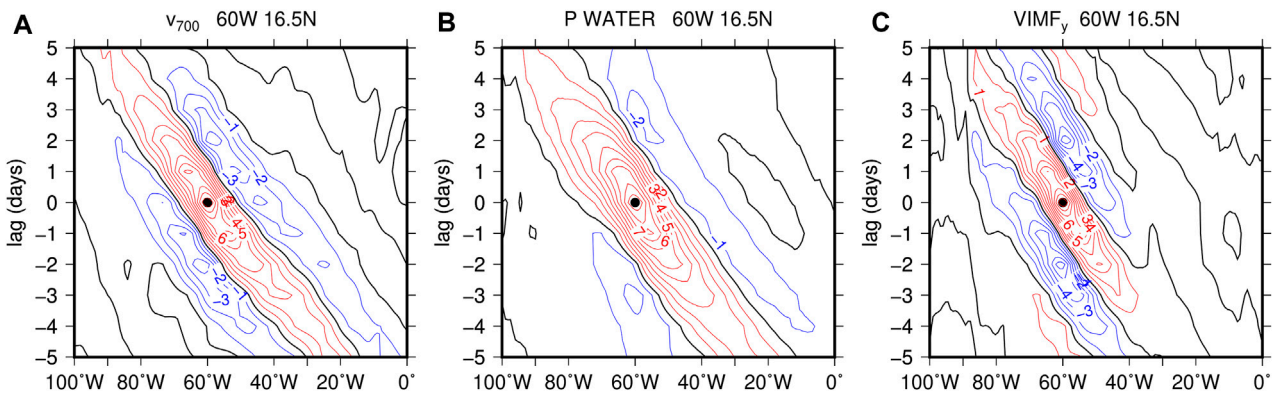

FIGURE 7
Modified time-longitude Hovmöller diagram for the 3–6 days band-pass filtered for **(A)** v_{700}, **(B)** PW and **(C)** $VIMF_y$, for the June-September period, with a reference point at 60°W, 16.5°N, red (blue) lines indicate positive (negative) correlations.

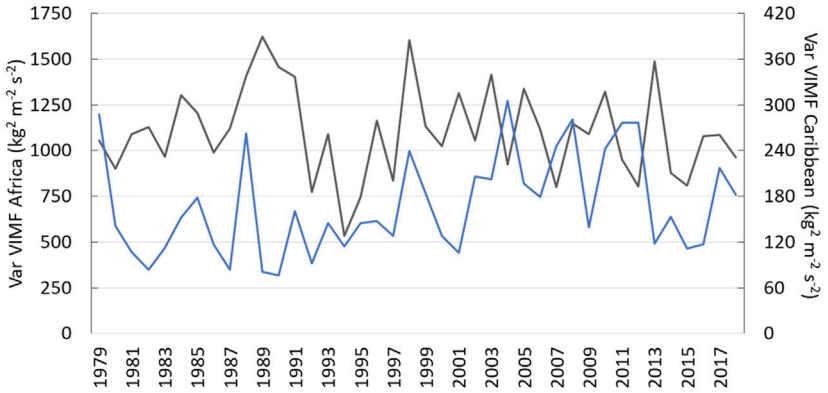

FIGURE 8
High-frequency (3–6 days period) variance of $VIMF_y$ during summer (June-September) for the years between 1979 and 2018, as a measure of African wave (grey line) and Caribbean EW (blue line) activity. The reference point for Africa is at 15°W, 18°N, and at 75°W, 16.5°N for the Caribbean Sea.

reflect the amplitude of high frequency transients, but not necessarily the number of these tropical perturbations.

By means of spectral analyses for the summer months, it is observed that the dominant mode of high-frequency variability in v_{700}, PW or $VIMF_y$ in the central Caribbean region corresponds to the frequency range of EWs (Figure 5). The v_{700} power spectrum at 75°W, 16.5°N shows a significant variance in the period range between 3 and 6 days (frequency between 0.17 and 0.33 $days^{-1}$) (Figure 5A). Spectral peaks in the frequency range 0.35 and 0.16 day^{-1} are observed in the power spectrum of PW (Figure 5B). Significant high-frequency variability in $VIMF_y$ occurs in the period range between 0.23 and 0.18 day^{-1} (Figure 5C). All these signals reflect the characteristic period of EW. Throughout the rest of this paper, the 3–6 days variance in $VIMF_y$ is used as a measure of EW activity.

The monthly total and high frequency variances in v_{700}, PW, or $VIMF_y$ indicate that EW activity over the Caribbean Sea is a dominant form of variability during the summer months. For instance, the 3–6 days variance of v_{700} is large between July and September and explains the largest percentage of the total variance (Figure 6A), more than 40%, particularly in July and August. The high-frequency variance in PW is also larger from June to August and explains more than 25% of the total variance (Figure 6B). The total and the high frequency variance in $VIMF_y$ tend to be low during the summer months, but the explained variance by high frequency transients, related to EWs, is larger between July and September (>35%) making them the dominant mode of variability in this region (Figure 6C), even while smaller than in the African and Atlantic tropical regions. In summary, the variance in $VIMF_y$ in summer months, mainly related to EW activity, is also the dominant form of high-frequency variability over the Caribbean Sea and consequently, climatologies on this phenomenon should reconsider their importance over the IAS.

EW propagation across the Atlantic Ocean

As suggested by Kerns et al. (2008), not all perturbations identified with vorticity maxima coming from Africa develop

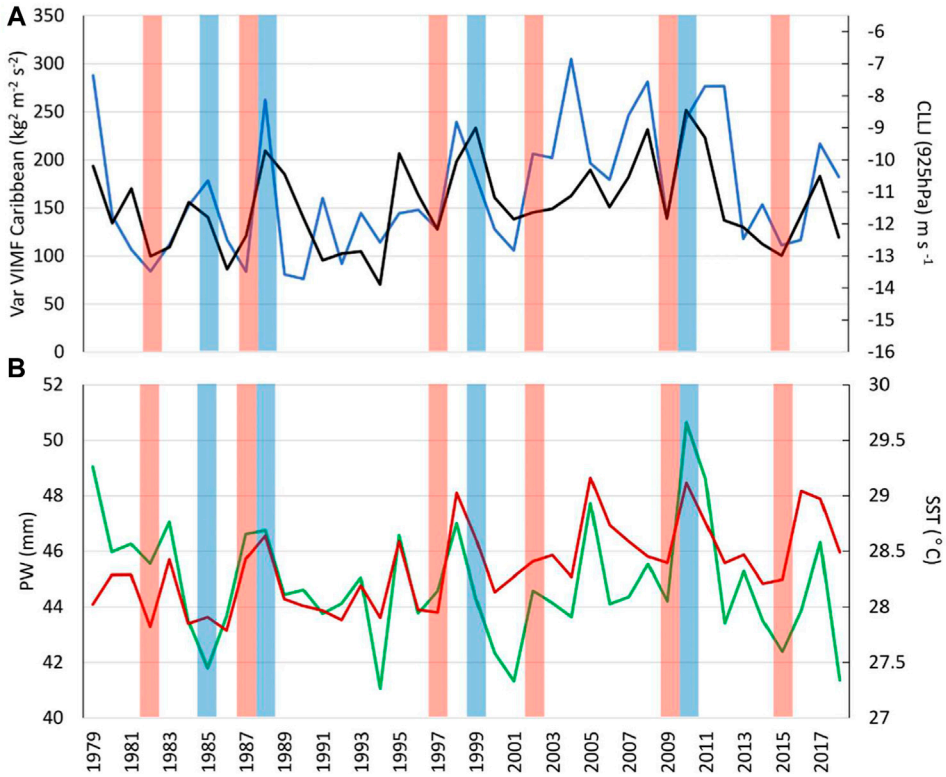

FIGURE 9
Mean seasonal (June-September) **(A)** Caribbean EW activity (blue line), zonal wind at 925 hPa over the central Caribbean (75°W, 15°N) as an index of the CLLJ (black line); **(B)** PW (mm) (green line) and SST (°C) (red line) over the central Caribbean. The red (light blue) vertical bars correspond to summer periods of El Niño (La Niña).

into EWs that reach the Caribbean Sea. The westward propagation of EWs across the Atlantic may be determined by means of a modified time-longitude Hovmöller diagram (Fraedrich and Lutz, 1987) of high frequency variations in v_{700}, PW or VIMF (Figure 7). Using the eastern Caribbean Sea (60°W, 16.5°N) as a reference point, for lags between −5 and +5 days, it is observed that the signal of EWs extends across most of the Atlantic, from around 20°W and into Central America (90°W). The waves signal, further downstream into the eastern Pacific, is not observed. The analyses also show that the wavelength of the tropical perturbations is of the order of 3,000 km with a phase speed of the order around 6 m·s^{-1}, which corresponds to the characteristic values of EWs in the Atlantic (Wang, 2015).

African easterly waves act as precursors for EW activity over the Caribbean Sea, but their amplification in this region may be related to quasi-stationary conditions such as (i) the barotropically unstable CLLJ (Molinari et al., 1997); or (ii) thermodynamic conditions, such as SSTs above 28°C and large atmospheric moisture availability (PW above 40 mm) that enhance convective activity over the Caribbean warm pool. The connection of the African easterly waves signal (around 0°) to the EW signal over the Caribbean is not evident in any of the three variables used to characterize these modes. V_{700} and $VIMF_y$ show that at around 16.5°N, EWs are present throughout most of the summer months, but contrary to what was suggested by Serra et al. (2010) their signal does not appear to extend into the eastern tropical Pacific.

EW activity over the IAS

Year to year variations in EW activity may have an important influence on the summer rainy season over the tropical Americas (Méndez and Magaña, 2010). High frequency variance of $VIMF_y$ may be used to analyze EW interannual variability (Figure 8) and its relationship with boundary conditions, such as SST or the mean flow, such as the intensity of the CLLJ, and to some extent, to African easterly wave activity. High-frequency variance in $VIMF_y$ appears to be an adequate measure of internnual African wave activity as it is coherent with other estimates of EW interannual variability, as those presented by Thorncroft and Hodges (2001). The high frequency variance in $VIMF_y$, off the western coast of Africa, is at least four times larger than over the Caribbean Sea. Even more, African wave activity and EW activity in the Caribbean are not significantly correlated ($r = 0.07$) which suggests that there are other factors controlling the latter. It is possible that EW activity over the IAS is related to the intensity of the CLLJ, to PW or the SST anomalies.

An analysis of high frequency variability in $VIMF_y$ shows that EW activity over the Caribbean Sea is related to a relatively weak CLLJ ($r = -0.6$), warm SSTs and high levels of PW ($r = 0.4$) (Figure 9). The interannual variations in summer PW and SSTs are correlated ($r = 0.5$) and their fluctuations are in turn, modulated by the intensity of the CLLJ, since an anomalously intense (weak) atmospheric low level zonal flow tends to result in anomalously cool

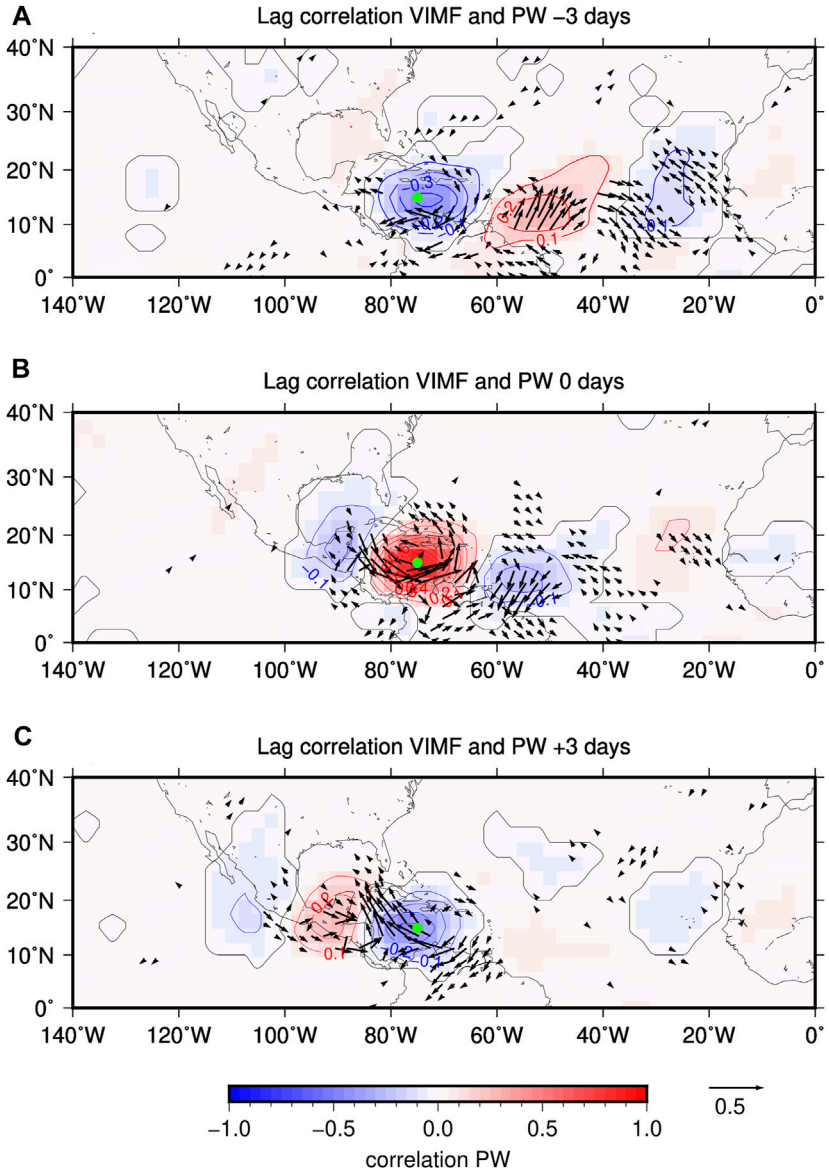

FIGURE 10
Lagged-cross correlations (significant at the 95%), between PW in the central Caribbean Sea (green dot) and PW and VIMF (vectors) in the tropical Atlantic and IAS region, from June to September for **(A)** lag = −3 days, **(B)** lag = 0 days and **(C)** lag = +3 days.

(warm) SSTs. Maxima in EW activity in the Caribbean occur in 1979, 1988, 1998, 2008, and 2017, which mostly correspond to La Niña conditions (Figure 9A). Weak EW activity occurs in 1986, 1992, 1994, 1997, 2000, and 2015, which mostly correspond to El Niño conditions and stronger than normal CLLJ. Therefore, on interannual time scales, SST, PW and the CLLJ intensity are correlated with EW activity over the Caribbean Sea and El Niño/Southern Oscillation (ENSO).

A strong CLLJ also results in an intense vertical wind shear that inhibits deep tropical convection (DeMaria, 1996; Herrera et al., 2015). This could also affect and reduce EW activity in a similar manner as TC activity is modulated by changes in the mean vertical wind shear between El Niño and La Niña years (Lin et al., 2020). The reduction in EW or TC activity contribute to reduce intense tropical convection over the Caribbean Sea (Taylor et al., 2002), and consequently result in dry years in the region.

EWs and intense precipitation events

Various studies show that intense EWs propagate across the Atlantic into the Yucatan Peninsula, the Gulf of Mexico and central southern Mexico, inducing low-level moisture convergence, ascending motion, and convective activity (e.g., Ladwig and Stensrud, 2009). This may be shown by means of one-point lagged-correlations between band-pass filtered 3–6 days anomalies of PW in the central Caribbean (75°W, 16°N), and the VIMF and PW across the tropical region, for

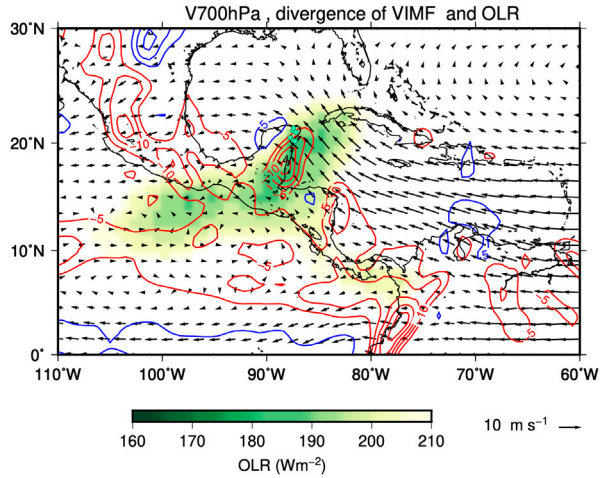

FIGURE 11
Composite pattern of the wind field at 700 hPa (vectors in m s^{-1}), the divergence (blue lines) and convergence (red lines) of VIMF (mm day^{-1}) and OLR below 210 Wm^{-2} (shades of green), when precipitation is above 30 mm day^{-1} in at least three out of six weather stations in the eastern part of the Yucatan Peninsula (green dots) for the period June-September between 1979–2018. The composite does not include days of intense precipitation associated with TCs, Some studies suggest that the westward EW propagation continues and reaches the Mexican Pacific coast and the Gulf of California to enhance the North American Monsoon convective activity (Adams and Stensrud, 2007). The use of VIMF may provide information on how the EW moisture packet may induce active periods in the monsoon.

lags −3, 0, and +3 days (Figure 10). The analysis shows that 3 days prior to a maximum in PW over the central Caribbean (Figure 10A) an EW like structure is observed over the Caribbean. The sequence of positive-negative correlations in VIMF anomalies (VIMF cyclonic and anticyclonic circulations) resembles Figure 1B, with a wavelength of around 3,000 km. The lag −3 correlations with PW shows a series of positive and negative correlations with PW over the Atlantic. The VIMF vortices associated with EWs propagate from the coast of Africa towards the IAS, almost in phase with a negative (positive) anomaly of PW, as in the traditional EW model (Riehl, 1954). The 0 days lag correlation shows a cyclonic circulation in phase with a positive PW anomaly over the central Caribbean (Figure 10B). The sequence of cyclonic-anticyclonic vortices of VIMF and positive-negative correlations with PW propagate from the Central Atlantic to southern Mexico and into the Yucatan Peninsula, with a northwestward propagation towards the Gulf of Mexico, following the mean flow associated with the CLLJ. The +3 days lagged correlation shows that the wave reaches southern Mexico and extends to the eastern Pacific (Figure 10C), as shown by Fuller and Stensrud (2000). The structure of vortices in the VIMF field is related to an EW is present over most of the Caribbean and southern Mexico. The anticyclonic vortex in the VIMF and negative correlation indicates diminished PW over the central Caribbean 2 days after its passage over the central Caribbean.

The previous analysis shows that the direction of propagation and extent of an EW may well affect most of the Caribbean Sea as well as Mexico, making this type of tropical wave an important moisture producing synoptic scale system during summer. The induced increases in PW frequently result in intense precipitation events as in the Yucatan peninsula.

EWs moisture convergence may lead to intense precipitation (>30 mm day^{-1}) in parts of the IAS. A composite pattern of the wind field at 700 hPa, VIMF convergence and OLR (below 210 Wm^{-2}) when intense precipitation (pcp > 30 mm day^{-1}) events in the eastern part of the Yucatan peninsula (Figure 11) shows the presence of an EW. The composite field corresponds to days when the precipitation over 30 mm day^{-1} is measured in at least three out of six weather stations (green dots), without including days of intense precipitation associated with TCs. The wavelength of the resulting EW pattern is of the order of 3,000 km and the most intense tropical convection (OLR < 210 Wm^{-2}) occurs east of the axis of the inverted trough, where intense convergence of VIMF (up to −20 mm day^{-1}) is observed. The passage of an EW over the Yucatan Peninsula implies the movement of a kind of "moisture packet" in the VIMF field, along with ascending motion that results in enhanced tropical convection.

Summary and conclusion

EW activity is a dominant form of high frequency variability in the IAS regions, contrary to what some climatologies appear to suggest. Although less energetic than their counterpart off the western coast of Africa, EWs over the IAS are frequent and modulate tropical local convection in a region where their ascending motions are important to counterbalance the dominant intense subsidence.

The summer rainy season over Mexico, Central America, and the Caribbean exhibits large intraseasonal and interannual fluctuations that may depend on the high frequency transient activity related to EWs. The interaction between EWs and the CLLJ is important to explain a good or bad rainy EW season. Strong EWs propagate across the Atlantic and reach the central Caribbean, where they frequently deflect into the Yucatan Peninsula. In this region, the passage of an EW and the associated moisture convergence may induce intense precipitation events of more than 30 mm day^{-1}.

EW activity over the Caribbean Sea tends to increase under a relatively weak CLLJ, as during La Niña years, since this condition tends to result in warmer SSTs and more humid atmospheric conditions over the Caribbean, and probably a weaker vertical wind shear that allows the development of deep tropical convection. On the contrary, an anomalously intense CLLJ tends to inhibit the development of deep tropical convection in the EW which reflects in anomalously low EW activity. From this perspective, the intensity of the CLLJ becomes a key factor to explain years of intense or weak EW activity and rains in the central southern part of Mexico.

Given that EWs act as "moisture packets" that induce intense precipitation they may constitute a mechanism that induces intense precipitation in other parts of Mexico. This is an interesting aspect of the relationship between EWs and storms that has been known by experienced meteorologists in the region. The dynamics of this

process is worth exploring. In this way, the present results may serve to determine the likelihood of intense precipitation even when there are no TCs present. Monitoring the "moisture packets" associated with EWs by looking at the daily soundings of wind and moisture content across the IAS region may serve to predict intense precipitation events. The National Hurricane Center Upper-Air Time Section Analyses (https://www.nhc.noaa.gov/index_station.shtml) are valuable sources of information.

On interannual time scales, climate outlooks of EW activity may be prepared based on the expected condition of the CLLJ and atmospheric moisture conditions in the tropical Atlantic, providing a hint on the likelihood of a relatively wet or dry summer season over Mexico, Central America and the IAS region. It is not only the intensity of the CLLJ what is of relevance for an outlook of this kind, but also its dominant direction into the Gulf of Mexico or the eastern tropical Pacific, since, as suggested by Méndez and Magaña (2010), this quasi-stationary circulation appears to act as a wave guide for EWs. In any event, the transient mean flow interaction process associated with EWs and the CLLJ should be further explored to determine the conditions that favor the amplification of EWs in a barotropically instability process, as these transients pass over the central Caribbean region.

Data availability statement

The raw data supporting the conclusion of this article will be made available by the authors, without undue reservation.

Author contributions

All authors contributed to the study conception and design. Figures preparation, data collection and analysis were performed by VM, EH, and MP. The first draft of the manuscript was written by VM and all authors commented on previous versions of the manuscript. All authors contributed to the article and approved the submitted version.

Funding

This study was funded by the CONAHCYT Grant PCC-319779 and DGAPA IA105123.

Acknowledgments

A valuable scientific discussion was conducted with Nuria Vargas and Sonia Díaz. The technical support of Gustavo Vázquez is highly appreciated. We also thank the support of the Instituto de Ciencias de la Atmósfera y Cambio Climático and the Instituto de Geografía, UNAM. Comments by two reviewers are appreciated.

Conflict of interest

The authors declare that the research was conducted in the absence of any commercial or financial relationships that could be construed as a potential conflict of interest.

Publisher's note

All claims expressed in this article are solely those of the authors and do not necessarily represent those of their affiliated organizations, or those of the publisher, the editors and the reviewers. Any product that may be evaluated in this article, or claim that may be made by its manufacturer, is not guaranteed or endorsed by the publisher.

References

Adams, J. L., and Stensrud, D. J. (2007). Impact of tropical easterly waves on the North American monsoon. *J. Clim.* 20 (7), 1219–1238. doi:10.1175/JCLI4071.1

Avila, L. A., Pasch, R. J., Beven, J. L., Franklin, J. L., Lawrence, M. B., Stewart, S. R., et al. (2003). Eastern North pacific hurricane season of 2001. *Mon. Weather Rev.* 131 (1), 249–262. doi:10.1175/1520-0493(2003)131<0249:ASNPHS>2.0.CO;2

Banacos, P. C., and Schultz, D. M. (2005). The use of moisture flux convergence in forecasting convective initiation: Historical and operational perspectives. *Wea. Forecast.* 20, 351–366. doi:10.1175/WAF858.1

Belanger, J. I., Jelinek, M. T., and Curry, J. A. (2016). A climatology of easterly waves in the tropical Western Hemisphere. *Geosci. Data J.* 3, 40–49. doi:10.1002/gdj3.40

Burpee, R. W. (1974). Characteristics of north african easterly waves during the summers of 1968 and 1969. *J. Atmos. Sci.* 31 (6), 1556–1570. doi:10.1175/1520-0469(1974)031<1556:conaew>2.0.co;2

Burpee, R. W. (1972). The origin and structure of easterly waves in the lower troposphere of north Africa. *J. Atmos. Sci.* 29, 77–90. doi:10.1175/1520-0469(1972)029<0077:TOASOE>2.0.CO;2

Camberlin, P., Kpanou, M., and Roucou, P. (2020). Classification of intense rainfall days in southern west Africa and associated atmospheric circulation. *Atmosphere* 11 (2), 188. doi:10.3390/atmos11020188

Carlson, T. N. (1969). Synoptic histories of three African disturbances that developed into Atlantic hurricanes. *Mon. Weather Rev.* 97 (3), 256–276. doi:10.1175/1520-0493(1969)097<0256:shotad>2.3.co;2

Cifelli, R., Lang, T., Rutledge, S. A., Guy, N., Zipser, E. J., Zawislak, J., et al. (2010). Characteristics of an African easterly wave observed during NAMMA. *J. Atmos. Sci.* 67 (1), 3–25. doi:10.1175/2009JAS3141.1

CONAGUA (2023). Datos climatología. Available at: https://smn.conagua.gob.mx/es/climatologia.

DeMaria, M. (1996). The effect of vertical shear on tropical cyclone intensity change. *J. Atmos. Sci.* 53, 2076–2088. doi:10.1175/1520-0469(1996)053<2076:TEOVSO>2.0.CO;2

Diedhiou, A. S., Janicot, A., Viltard, P., de Felice, P., and Laurent, H. (1999). Easterly wave regimes and associated convection over west Africa and tropical atlantic: Results from the NCEP/NCAR and ECMWF reanalyses. *Clim. Dyn.* 15, 795–822. doi:10.1007/s003820050316

Domínguez, C., and Magaña, V. (2018). The role of tropical cyclones in precipitation over the tropical and subtropical north America. *Front. Earth Sci.* 6, 19. doi:10.3389/feart.2018.00019

Ejigu, Y. G., Teferle, F. N., Klos, A., Bogusz, J., and Hunegnaw, A. (2021). Monitoring and prediction of hurricane tracks using GPS tropospheric products. *GPS Solut.* 25, 76. doi:10.1007/s10291-021-01104-3

Enyew, B. D., and Mekonnen, A. (2022). The interaction between african easterly waves and different types of deep convection and its influence on atlantic tropical cyclones. *Atmosphere* 13 (1), 5. doi:10.3390/atmos13010005

Fasullo, J., and Webster, P. J. (2003). A hydrological definition of Indian monsoon onset and withdrawal. *J. Clim.* 16 (19), 3200–3211. doi:10.1175/1520-0442(2003)016<3200a:ahdoim>2.0.co;2

Fraedrich, K., and Lutz, M. (1987). A modified time-longitude diagram applied to 500 mb heights along 50° north and south. *Tellus A Dyn. Meteorol. Oceanogr.* 39, 25–32. doi:10.3402/tellus.a.v39i1.11736

Frank, N. L. (1970). Atlantic tropical systems of 1969. *Mon. Wea. Rev.* 98, 307–314. doi:10.1175/1520-0493(1970)098<0307:ATSO>2.3.CO;2

Frank, N. L. (1969). The "inverted v" cloud pattern—An easterly wave? *Mon. Weather Rev.* 97, 130–140. doi:10.1175/1520-0493(1969)097<0130:tvcpew>2.3.co;2

Fuller, R. D., and Stensrud, D. J. (2000). The relationship between tropical easterly waves and surges over the Gulf of California during the North American monsoon. *Mon. Weather Rev.* 128 (8 II), 2983–2989. doi:10.1175/1520-0493(2000)128<2983:trbtew>2.0.co;2

Gomes, H. B., Ambrizzi, T., Herdies, D. L., Hodges, K., and Pontes da Silva, B. F (2015). Easterly wave disturbances over northeast Brazil: An observational analysis, *Adv. Meteorology* 2015, 1–20. doi:10.1155/2015/176238

Herrera, E., Magaña, V., and Caetano, E. (2015). Air-sea interactions and dynamical processes associated with the midsummer drought. *Int. J. Climatol.* 35, 1569–1578. doi:10.1002/joc.4077

Hodges, K. I., Hoskins, B. J., Boyle, J., and Thorncroft, C. (2003). A comparison of recent reanalysis datasets using objective feature tracking: Storm tracks and tropical easterly waves. *Mon. Weather Rev.* 131 (9), 2012–2037. doi:10.1175/1520-0493(2003)131<2012:acorrd>2.0.co;2

Hosler, C. R. (1956). A study of easterly waves in the Gulf of Mexico. *Bull. Am. Meteorol. Soc.* 37 (3), 101–107. doi:10.1175/1520-0477-37.3.101

Kerns, B., Greene, K., and Zipser, E., (2008) Four years of tropical ERA40 vorticity maxima tracks. Part I: Climatology and vertical vorticity structure. *Mon. Wea Rev.* 136, 4301–4319. doi:10.1175/2008MWR2390.1

La revista Peninsular (2023). Tren de ondas tropicales se aproxima a la península. Available at: https://www.larevista.com.mx/yucatan/tren-de-ondas-tropicales-se-aproxima-a-la-peninsula-15691.

Ladwig, W. C., and Stensrud, D. J. (2009). Relationship between tropical easterly waves and precipitation during the North American monsoon. *J. Clim.* 22 (2), 258–271. doi:10.1175/2008JCLI2241.1

Lawton, Q. A., Majumdar, S. J., Dotterer, K., Thorncroft, C., and Schreck, C. J. (2022). The influence of convectively coupled kelvin waves on african easterly waves in a wave-following framework. *Mon. Wea. Rev.* 150, 2055–2072. doi:10.1175/MWR-D-21-0321.1

Liebmann, B., and Smith, C. A. (1996). Description of a complete (interpolated) outgoing Longwave radiation dataset. *Bull. Amer Meteorol. Soc.* 77, 1275–1277.

Lin, I.-I., Camargo, S. J., Patricola, C. M., Boucharel, J., Chand, S., Klotzbach, P., et al. (2020). "ENSO and tropical cyclones," in *El Niño southern oscillation in a changing climate*. Editors M. J. McPhaden, A. Santoso, and W. Cai (Hoboken, New Jersey: John wiley). doi:10.1002/9781119548164.ch17

Magaña, V., and Diaz, S. (2022). Inter- Ocean basin moisture fluxes and the onset of the summer rainy season over southern Mexico. *Front. Clim.* 4, 1037350. doi:10.3389/fclim.2022.1037350

Magaña, V., and Yanai, M. (1991). Tropical-midlatitude interaction on the time scale of 30 to 60 days during the northern summer of 1979. *J. Clim.* 4 (2), 180–201. doi:10.1175/1520-0442(1991)004<0180:tmiott>2.0.co;2

Maul, G. A. (2008). "Intra-Americas Sea," in *Encyclopedia of ocean sciences* (Cambridge, Massachusetts: Academic Press), 286–294. doi:10.1016/B978-012374473-9.00380-5

Méndez, M., and Magaña, V. (2010). Regional aspects of prolonged meteorological droughts over Mexico and Central America. *J. Clim.* 23, 1175–1188. doi:10.1175/2009JCLI3080.1

METED (2023). Available at: https://www.meted.ucar.edu/tropical/synoptic/Afr_E_Waves/ (Accessed April 30, 20239).

Molinari, J., Knight, D., Dickinson, M., Vollaro, D., and Skubis, S. (1997). Potential vorticity, easterly waves, and eastern Pacific tropical cyclogenesis. *Mon. Weather Rev.* 125 (10), 2699–2708. doi:10.1175/1520-0493(1997)125<2699:PVEWAE>2.0.CO;2

Molinari, J., Vollaro, D., Skubis, S., and Dickinson, M. (2000). Origins and mechanisms of eastern pacific tropical cyclogenesis: A case study. *Mon. Weather Rev.* 128 (1), 125–139. doi:10.1175/1520-0493(2000)128<0125:oamoep>2.0.co;2

Murakami, M. (1979). Large-scale aspects of deep convective activity over the GATE area. *Mon. Weather Rev.* 107, 994–1013. doi:10.1175/1520-0493(1979)107<0994:lsaodc>2.0.co;2

Nitta, T. (1970). On the role of transient eddies in the tropical troposphere. *J. Meteorol. Soc. Jpn.* 48, 348–359. doi:10.2151/jmsj1965.48.4_348

Núñez Ocasio, K. M., and Rios-Berrios, R. (2023). African easterly wave evolution and tropical cyclogenesis in a pre-Helene (2006) hindcast using the Model for Prediction across Scales-Atmosphere (MPAS-A). *J. Adv. Model. Earth Syst.* 15, e2022MS003181. doi:10.1029/2022MS003181

Olafsdottir, K. B., Schulz, M., and Mudelsee, M. (2016). REDFIT-X: Cross-spectral analysis of unevenly spaced paleoclimate time series. *Comput. Geosci.* 91, 11–18. doi:10.1016/j.cageo.2016.03.001

Palmer, C. E. (1952). Reviews of modern meteorology-5. Tropical meteorology. *Q. J. R. Meteorol. Soc.* 78, 126–164. doi:10.1002/qj.49707833603

Reed, R. J., Klinker, E., and Hollingsworth, A. (1988). The structure and characteristics of African easterly wave disturbances as determined from the ECMWF operational analysis/forecast system. *Meteorl Atmos. Phys.* 38, 22–33. doi:10.1007/BF01029944

Reed, R. J., Norquist, D. C., and Recker, E. E. (1977) The structure and properties of african wave disturbances as observed during phase III of GATE. *Mon. Weather Rev.* 105:317–333. doi:10.1175/1520-0493(1977)105<0317:tsapoa>2.0.co;2

Riehl, H. (1979). *Climate and weather in the tropics*. Cambridge, Massachusetts: Academic Press, 611.

Riehl, H. (1948). On the formation of typhoons. *J. Atmos. Sci.* 5 (6), 247–265. doi:10.1175/1520-0469(1948)005<0247:otfot>2.0.co;2

Riehl, H. (1954). *Tropical meteorology*. New York: McGraw-Hill, 392.

Riehl, H. (1945). *Waves in the easterlies and the polar front in the tropics*. Chicago, Illinois: University of Chicago Misc. Rep., 79.

Seo, H., Jochum, M., Murtugudde, R., Miller, A. J., and Roads, J. O. (2008). Precipitation from african easterly waves in a coupled model of the tropical atlantic. *J. Clim.* 21 (6), 1417–1431. doi:10.1175/2007JCLI1906.1

Serra, Y. L., Kiladis, G. N., and Hodges, K. I. (2010). Tracking and mean structure of easterly waves over the Intra-Americas Sea. *J. Clim.* 23 (18), 4823–4840. doi:10.1175/2010JCLI3223.1

Shelton, K. (2011). *Easterly waves and tropical cyclogenesis in the Caribbean*. Ph D Thesis. New York: State University of New York at Albany, 306.

Suneetha, P., Latha, P., Rao, S., Zedek, D., Lakshmi, K., and Kumar, O. (2018). An easterly wave generated heavy rainfall event over south India-A case study. *Int. J. Geosci.* 9, 606–618. doi:10.4236/ijg.2018.910036

Tai, K., and Ogura, Y. (1987). An observational study of easterly waves over the eastern pacific in the northern summer using FGGE data. *J. Atmos. Sci.* 44 (2), 339–361. doi:10.1175/1520-0469(1987)044<0339:AOSOEW>2.0.CO;2

Taylor, M. A., Enfield, D. B., and Chen, A. A. (2002) Influence of the tropical atlantic versus the tropical pacific on caribbean rainfall, *J. Geophys. Res.*, 107(C9), 3127. doi:10.1029/2001JC001097

Thompson, R. M., Payne, S. W., Recker, E. E., and Reed, R. J. (1979). Structure and properties of synoptic-scale wave disturbances in the intertropical convergence zone of the eastern atlantic. *J. Atmos. Sci.* 36 (1), 53–72. doi:10.1175/1520-0469(1979)036<0053:saposs>2.0.co;2

Thorncroft, C., and Hodges, K. (2001). African easterly wave variability and its relationship to atlantic tropical cyclone activity. *J. Clim.* 14 (6), 1166–1179. doi:10.1175/1520-0442(2001)014<1166:aewvai>2.0.co;2

Wang, Z. (2015). "Tropical cyclones and hurricanes. Tropical Cyclogenesis," in *Encyclopedia of atmospheric sciences* (Amsterdam, Netherlands: Elsevier), 57–64. Available at: https://www.sciencedirect.com/science/referenceworks/9780124095489.

Whitaker, J. W., and Maloney, E. D. (2020). Genesis of an east pacific easterly wave from a Panama bight mcs: A case study analysis from June 2012. *J. Atmos. Sci.* 77, 3567–3584. doi:10.1175/JAS-D-20-0032.1

Yanai, M., Maruyama, T., Nitta, T., and Hayashi, Y. (1968). Power spectra of large-scale disturbances over the tropical Pacific. *J. Meteor Soc. Jpn.* 46, 308–323. doi:10.2151/jmsj1965.46.4_308

Yanai, M., and Nitta, T. (1967). Computation of vertical motion and vorticity budget in a Caribbean easterly wave. *J. Meteor Soc. Jpn.* 45, 444–466. doi:10.2151/jmsj1965.45.6_444